Available online at www.most.gov.bd

Volume 04, Issue (1), Page: 145-154, 2022

Ministry of Science and Technology
Government of The People's of Bangladesh
Bangladesh Secretariat, Dhaka.

Synthesis and Characterization of Eco-friendly, Biodegradable Plasticized Starch Nanocomposite using Graphene Oxide Nano-filler for Energy Storage Applications

S. Islam. Mollik, E. Mahmud, M. F. Mina and M. R. Islam*

Department of Physics, Bangladesh University of Engineering and Technology (BUET), Dhaka, Bangladesh

Abstract

In this study, environment-friendly, biodegradable nanocomposite has been fabricated using plasticized starch (PS) polymer and graphene oxide (GO) nanofiller. Biodegradable PS has been extracted from potatoes and a solution casting technique was used to synthesize PS/GO nanocomposite. The structural and surface morphological properties of the nanocomposite have been studied via FTIR and FESEM which demonstrate increased degree of interaction between the PS matrix and the GO nanofiller. The thermal properties of the nanocomposite showed that incorporation of GO improves the thermal stability of the nanocomposites. To study the energy storage capabilities of the PS/GO nanocomposites the electrochemical properties of the nanocomposites were as studied through cyclic voltammetry (CV), and galvanostatic charge-discharge (GCD) methods. The PS/GO nanocomposite showed improved capacitive performance with a specific capacitance of 112 F/g compared to that of pure starch (2.20 F/g) at a current density 0.1 mA/cm^2. To study the effect of GO on the electrochemical properties of the nanocomposites, electrochemical impedance spectroscopy was performed and the corresponding graphs were simulated using simulation software. The incorporation of GO reduces the charge transfer resistance and thereby improve the capacitive performance. The improved electrochemical performance of the PS/GO nanocomposite can be further attributed to the large surface areas provided by the GO sheets allowing faster transport of electrolyte ions into the electrode. The result indicates that the PS/GO and nanocomposites may offer a promising route for the synthesis of bio-friendly and flexible energy storage devices.

Received: 26.09.2022
Revised: 27.03.2023
Accepted: 10.05.2023

DOI: https://doi.org/10.3329/jscitr.v4i1.67376

Keywords: Biodegradable; Plastics; Nanocomposite; Graphene oxide; Nano-filter.

Introduction

Plastic is considered one of the most significant innovations of the 20th century because of its resilience against degradability, flexibility, ease of manufacture, imperviousness to water, and cost-effectiveness are used in lots of products of different sizes, from paper clips to spacecraft. Plastic has replaced traditional materials, such as wood, stone, horn, bone, leather, metal, glass, and ceramic. But this wonder-product, which has transformed our lives in so many positive ways, has severe environmental flaws in its production and disposal and has become a significant concern for human health and the environment.

*Corresponding author's e-mail: rakibul@phy.buet.ac.bd

Bio-nanocomposites offer an environment-friendly strategy for the production of novel materials and have the potential to replace conventional plastic. These systems comprise a continuous biopolymer matrix loaded with nanofillers, usually inorganic (Thomas *et al.,* 2015; Dang *et al.,* 2013; Li *et al.,* 2020). While the biopolymer matrix ensures the material's biodegradability, nanofillers provide the required thermal, mechanical, and electrical properties, usually very poor in the biopolymer alone (Kim *et al.,* 2008; Khurram *et al.,* 2015). Although polymer goes through a recycling process, a small proportion is actually remade into materials. Many other reasons motivate industries and researchers to find alternatives to non-renewable resources; however, all replacements for current plastics should meet some essential conditions; they need to be low-cost, renewable, sustainable, and biodegradable Dang *et al.,* 2012; Ge *et al.,* 2017.

Among different biopolymers, starch is a very popular polymar because of its cost-effectiveness as it can be easily obatined from natural sources such as vegetables and cereals. Besides the nutritional value, the film-forming ability has given starch a more notable role; for example, they found their applications in food packaging. Starch-based films are biodegradable and edible and, therefore, potential substitutes for many synthetic packaging materials and pose little harm to the environment. Unfortunately, starch-based biocomposites exhibit many disadvantages (e.g., strong hydrophilic character, poor mechanical properties, and low thermal stability) compared to conventional polymers, which make them unsatisfactory for practical applications (Maa *et al.,* 2013; Geng *et al.,* 2014; Ciszewski *et al.,* 2015). Moreover, nano-sized fillers can also increase dispersibility in polymer resin and improve mechanical, thermal, and dielectric properties Bera *et al.,* 2017; Díez-Pascual *et al.,* 2018.

The nanometer-scale fillers are often introduced into a plasticized starch (PS) matrix to improve the physical properties of the polymer. Recently, carbon-based materials have been used as fillers for PS-based composites. Carbon nanotube (CNT) has been incorporated into the PS matrix to enhance the polymer's tensile strength and electrical conductivity. Carbon black was added to the PS matrix to obtain electrically conductive composites prepared by melt extrusion and microwave radiation. The composites prepared using microwave radiation exhibited better properties, including reinforcing effect, conductivity, and water vapor barrier than those from melt extrusion. Graphene, a two-dimensional sheet of carbon exfoliated from graphite, has recently emerged as one of the most popular and unique filler materials because of its excellent chemical and physical characteristics. Graphene also provides a large surface area, high thermal and electrical conductivity, and extraordinary mechanical properties. Because of these properties, graphene find its applications in diverse fields, including field effect transistor, memory device, hydrogen storage, conducting electrode, ultra-capacitor, and solar cell Yousefi *et al.,* 2013. Several studies have demonstrated that graphene function as better nanofillers for polymer. The pristine graphene are very costly and challenging to synthesize, which reduces its applicability as nanofiller materials. On the contrary, a different form of graphene, graphene oxide (GO), contains reactive functional groups on the basal plane and edge, including hydroxyl, carboxyl, carbonyl, and epoxy. With these functional groups, GO possesses unique characteristics and various potential applications, such as good dispersion stability in water and other organic solvents and low manufacturing cost. These intrinsic properties of GO make it a suitable nanofiller for polymer matrix composite materials (Yousefi *et al.,* 2012, ; Kim *et al.,* 2007).

In this study PS/GO biocomposite films were prepared by the solution casting method. The aim of this work is to study the influence of GO loading on the structural, surface morphologic, and thermal properties of the PS. Fourier transform infrared spectroscopy (FTIR), Field emission scanning electron microscopy (FESEM), and thermal gravimetric analysis (TGA) analysis was performed to get study the surface morphological, thermal, and structural properties of PS/GO nanocomposite. The electrochemical proper-

ties of pure PS and GO/PS were fully characterized by cyclic voltammetry (CV), galvanostatic charge-discharge (GCD), and electrochemical impedance spectroscopy (EIS) analysis.

Experimental details

Extraction of starch

At first, potatoes were cleaned and cut into tiny pieces, mixing them with distilled water to form a paste. The mixed solution was then stirred for several hours. Then, the liquid portion of the potato juice was detached, leaving a fine mesh. It was then poured into a petri dish for a few hours at 30 ºC, leaving the starch to settle inside the pot. The as-prepared starch particle was washed several times in distilled water, followed by drying at 100 ºC in the oven. Fig-1 shows the schematic diagram of the extraction of starch from potatoes..

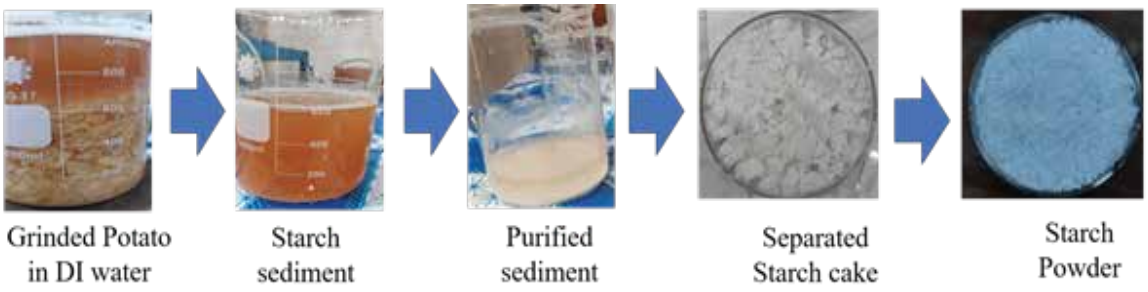

Fig. 1. Synthesis process of starch from plant derived source (potato).

Preparation of Graphene oxide

Graphene Oxide (GO) will be synthesized by modified Hummer's method. Graphite fine powder, Potassium Permanganate ($KMnO_4$), $NaNO_3$, H_2O_2, H_2SO_4 was used. H_2SO_4 was added to the mixture of Graphite and $NaNO_3$. After cooling, it was kept in an ice bath, and $KMnO_3$ was added slowly. The mixture was heated and stirred for a few hours, followed by adding DI water in an oil bath. H_2O_2 was added slowly, followed by continuous stirring. After ultrasonication, GO was heated with Hydrazine Hydrate at 100^0c for 6 hours. Hydrazine Hydrate acted as a reducing agent Bonardd *et al.,* 2019; Lin *et al.,* 2012; Fan *et al.,* 2012; Kumar *et al.,* 2015; Malmir *et al.,* 2018.

Preparation of starch- glycerin film

At first, the starch powder was dissolved in distilled water. 30 wt % glycerin was mixed with water in a vial and added slowly into the starch solution, followed by stirring. The mixed solution was then heated slowly in an oil bath at 70 ºC which allows for gradual evaporation of the solvent. Then the suspension was then poured onto a glass plate and kept inside an oven at 40 ºC.

Preparation of starch/GO nanocomposite

To break down the long chains of the starch polymer, vinegar was used. Propane-1, 2, and 3-triol (glycerol) were added to plasticize the starch. GO powder was sonicated for 15 minutes in DI water. The mixture of starch, vinegar, glycerol and GO will then be heated at 100 ^{0}C for 15 minutes. Then the mixture was poured onto a glass petri dish. After drying at 50 ºC in an oven will give GO/Starch nanocomposite film (Li *et al.,* 2011; Chandra *et al.,* 2010; Usman *et al.,* 2016; Jammula *et al.,* 2015; Maa *et al.,* 2013).

Characterization of starch/GO and starch/RGO nanocomposite

Various characterization methods were employed to study the properties of PS/GO nanocomposite. The chemical bonding properties of the nanocomposite were analyzed via an FTIR spectrometer (Nicolet 6700, Thermo Fisher). To study the surface morphology of the composite field emission scanning electron microscope (FESEM) images were taken at 5 kV using a JEOL-JSM 7600 microscope. Before imaging, a thin layer of gold was coated on the film surface via thermal evaporation. To study the thermal stability of PS/GO nanocomposites ththermalravimetric analysis (TGA) was performed using a TG50, Shimadzu machine. The TGA analysis was performed between 25 ºC and 800 ºC at a heating rate 10 ºC/min under a nitrogen atmosphere.

The electrochemical measurements were performed in 0.1M KCL solution by an electrochemical workstation (CS310, Corr Test Instrument Co. Ltd., China) at room temperature. A three electrode cell setup consisting of Ag/AgCl reference electrode, Glassy Carbon working electrode and platinum plate (1 × 1 cm^2) counter electrode was used for taking the data.

Results and Discussion

Chemical properties of PS/GO nanocomposite

To investigate the chemical changes that occur in PS due to the incorporation of GO nanofiller, ATR-FTIR spectroscopy were performed. Figure 2 shows the FTIR spectrum for PS and PS/GO nanocomposite. As seen from the FTIR spectrum of neat PS nanocomposite, the region at 2950-3450 cm^{-1} refers to hydroxyl groups (Xie *et al.,* 2013; Yao and Zhou 2015). Stretching and bonding of –OH groups occurred at 3352 cm^{-1} and 1651 cm^{-1} respectively. The presence of CH_2 groups determines the existence of peak at 2941 cm^{-1}. The bands at 1153 cm^{-1} and 1109 cm^{-1} were attributed to the stretching vibration of C–O in C–O–H groups and at 991 cm^{-1} stretching of C-O in C-O-C groups. In the spectrum of the PS/GO nanocomposite the O-H bending has been shifted from 1651 cm^{-1} to 1645 cm^{-1} which indicates formation of hydrogen bonding between

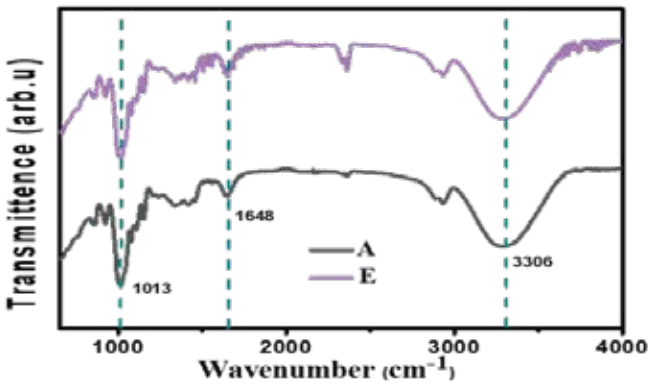

Fig. 2. FTIR spectra of PS/rGO nanocomposites with concentration of GO added to 0%, 0.5% and 1.0%.

GO and PS in the nanocomposite. Similar type of shift towards shorter wavenumbers has also been observed for most of the peak. Additionally, the intensity of the band corresponds to the O-H group (at 3352 cm^{-1}) increases with the incorporation of GO. This suggests that the GO enhance the affinity of water to the surface (Yao and Zhou 2015).

Surface morphology of the PS/GO nanocomposite

The SEM images of the fractured faces of PS and GO/PS composites are shown in the figure 3. GO sheets were observed to be uniformly dispersed in the PS matrix. In addition, GO appeared to be covered by the PS matrix, which was related to stronger interfacial interactions between GO and the matrix. GO sheets with more oxygen-containing groups could form better hydrogen bond interactions with starch. A layered structure caused by the incorporation of GO (Fig. 3b) was clearly observed in the cross-section of the films compared with the pure PS film (Lin *et al.,* 2012).

Thermal properties of PS/RGO nanocomposite

The thermal stability of PS and GO/PS films was performed by thermo gravimetric analysis (TGA) and is shown in Fig. 4 (a). Thermal analysis was performed in order to determine whether GO could produce

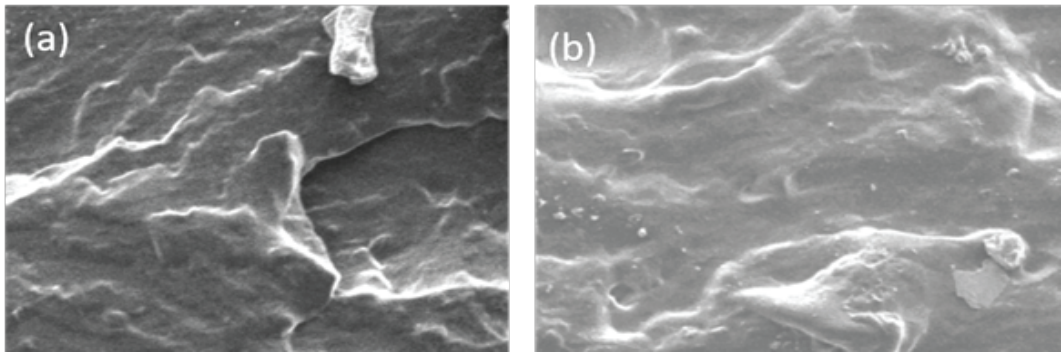

Fig. 3. FESEM images of the cross-sections of (a) PS and (b) PS/GO nanocomposites.

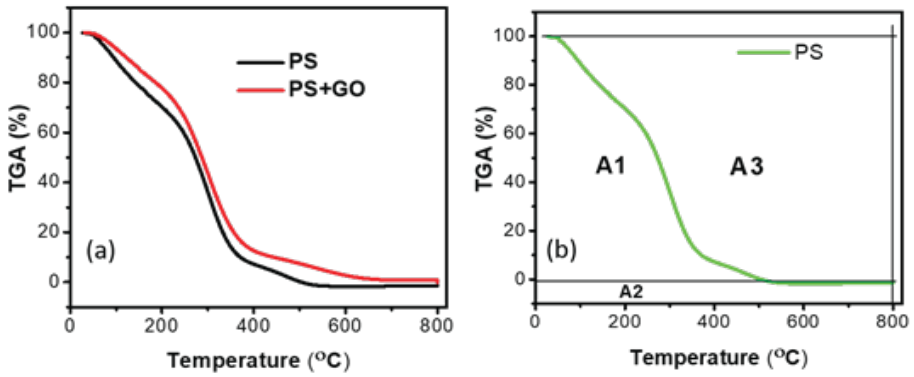

Fig. 4. (a) Effect of rGO loading on the thermal property of PS/rGO nanocomposite, (b) schematic representation of A1, A2, and A3 for A* and K*.

any change in the thermal decomposition behavior of starch. The onset temperatures of PS and GO/PS films are 242 ºC and 250 ºC, respectively. Onset temperature is the temperature when the first detectable heat is released, obtained by extrapolation of the steepest portion of the curve. The weight loss before the onset temperature was attributed to volatilization of water absorbed by the starch and

glycerol plasticizer (Yao and Zhou 2015). The second stage of the weight loss in the temperature range between 220 –380 ºC corresponded to the decomposition of starch. An improvement in the thermal stability of the nanocomposite films could be seen due to the incorporation of GO fillers. All the experimental results of TGA, which was generally accepted and used to assess the thermal stability such as the initial decomposed temperature (IDT), the integral procedural decomposition temperature (IPDT), the temperature at 50% weight loss (T−50%) and the temperature at the maximum rate of mass loss (T_{max}) are listed in table 1. It could be observed that the PS/GO nanocomposite showed a higher decomposition temperature than that of PS film. These results indicated that the decomposition temperatures of starch increased due to the addition of GO. In the presence of GO, the mobility of the PS chains got suppressed by strong hydrogen bonding interactions with GO. Usually, thermal stability relies on the interaction between the filler and the polymer matrix. From the Table-1, it is evident that the decomposition temperature of the nanocomposite increased due to the incorporation of the GO nanofiller.

The integral procedural decomposition temperature (IPDT) can be used to assess a material's lifetime. Fig. 4 (b) shows the calculation procedure of IPDT.

Table 1. Thermal properties of PS and PS/GO nanocomposite.

Sample	IDT	IPDT	T-50%	T_{max}
PS	242	242	270	380
PS+ GO	250	266	275	385

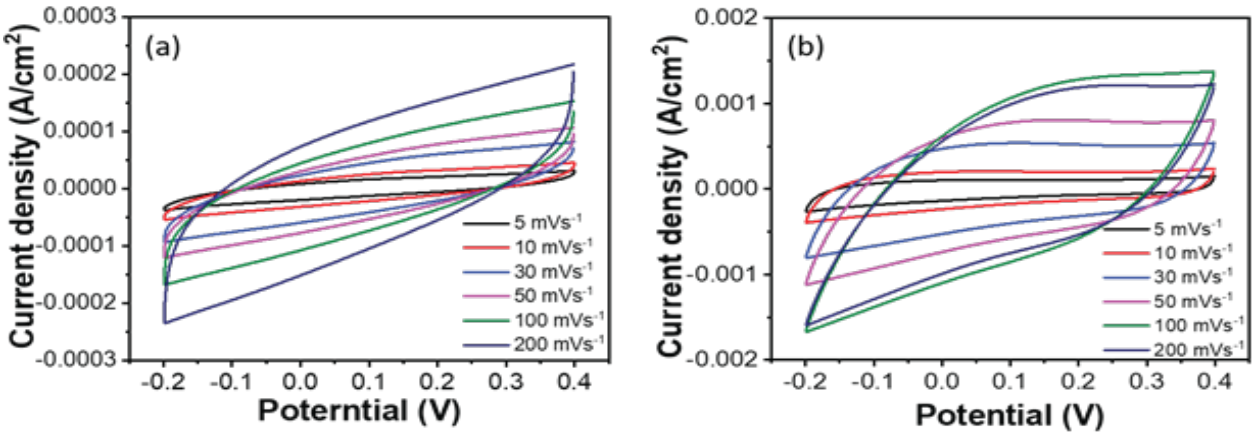

Fig. 5. Cyclic Voltammetry curves of (a) PS and (b) PS/GO(0.5%) electrodes at different scan rate.

The IPDT is calculated as follows [28]: $IPDT=A^*K^*(T_f-T_i)+T_i$

Where A^* is the area ratio of the total experimental curve divided by the total TGA thermo gram [$(A1 + A2)/(A1 + A2 + A3)$], K^* is the coefficient of A^*

[$(A1 + A2)/A1$], Ti is the initial experimental temperature (25 °C in this work), and $Tf$is the final experimental temperature (800 °C).

Electrochemical properties of PS/GO nanocomposite

To explore the effect of GO on the capacitative performance of the nanocomposite cyclic voltagrams (CV) were recorded. The CV measurements were performed at various voltage scan rate $5mVs^{-1}$, $10mVs^{-1}$, $20mVs^{-1}$, $30mVs^{-1}$,$50mVs^{-1}$, 100 $mVs^{-1}$and 200 mVs^{-1} in a potential window of 1V. The corresponding CV curves for PS and PS/GO composites are presented in figure 5 (a) and 5(b), respectively. The figure shows that the area of the CV curves increases with the increase of the scan rate (Xia *et al.,* 2017; Tian *et al.,* 2014). For all scan rates, the CV curves for PS exhibit a near rectangle cyclic voltammogram, whereas a distorted rectangular shape is observed for the PS/GO composite. Such deviation can be attributed to the pseudocapacitance originating from oxygen groups on the surface of the GO and presence of uncompensated resistance due to the GO flake in the system. Additionally, the cyclic voltammograms for GO, and GO/PS composite exhibit a sharp rise in current at a low voltage, which drops sharply at the vertex potential indicating the good electrochemical stability of the electrode material Zhu and Guo 2017; Nan *et al.,* 2010; Song *et al.,* 2016). The area of the CV curves is proportional to the specific capacitance of the electrode. From the figure, it is observed that the area of the CV curve increases when PS/GO nanocomposite is greater than that of the neat PS. This gives a qualitative idea that the specific capacitance of PS/GO is larger than that of PS. This result implied that GO played key role in speeding up carriers' transportation along the PS networking chains.

Fig. 6 shows the galvanostatic charge-discharge (GCD) curves of PS and PS/GO nanocomposite at different current densities. The PS/GO composite's discharge time is much longer than PS. It was observed that the charging/discharging curve significantly depends on the current densities and the charging/discharging time decreases with the increase of current density. This suggests that at low current density, the ions diffuse through the materials, whereas at higher current density, the movement of the ions through the composite is hindered (Zhu and Guo, 2017).

The specific capacitances of the different nanocomposites were estimated from their respective GCD curve using the formula (Cole and Cole 1941). $C_s = I\Delta t/m\Delta V$. Where I, t, V, and m are the constant current (A), discharge time (s), total potential deviation (V), and the mass of the active materials within the electrode (g), respectively. The specific capacitances of PS, and PS/GO composite electrodes were found to be 2.78 F/g, and 124 F/g, respectively.

Electrochemical impedance analysis (EIS) was also performed to determine the cause for improving the electrochemical performance of the PS/GO nanocomposite. Fig. 7 (a) and (b) represent the EIS curve for PS and PS/GO. Each curve contains a semicircular region at a high-frequency range and a straight portion at a low frequency. Both curves were simulated using the Z-view software following an AC circuit. The simulation gives the value of solution resistance (R_s) and the charge transfer resistance (R_{ct}). The values of Rs and Rct obtained from the simulation of EIS data are repented in table-2. The incorporation of GO reduces the charge transfer resistance from 4.5 k Ohm to 1.9 k Ohm. Incorporating GO improves the polymer's charge transfer resistance and improves the capacitances.

These data suggest the significantly enhanced specific capacitances of PS/GO nanocomposite originating from the synergistic effect of PS and GO. Such an enhancement in capacitance can be attributed to several factors. GO with a higher specific surface area increases the effective interfacial area between the nanocomposite and electrolyte. In contrast, GO's layered structure reduces the electrolyte ions' diffusion length. This improves the specific capacitance by increasing the electroactive region. Additionally, due to

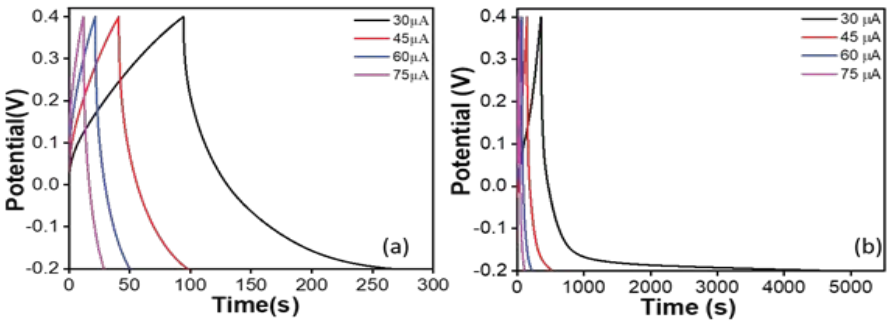

Fig. 6. Cyclic Voltammetry curves of PS, and PS/GO electrodes at different sweep rate.

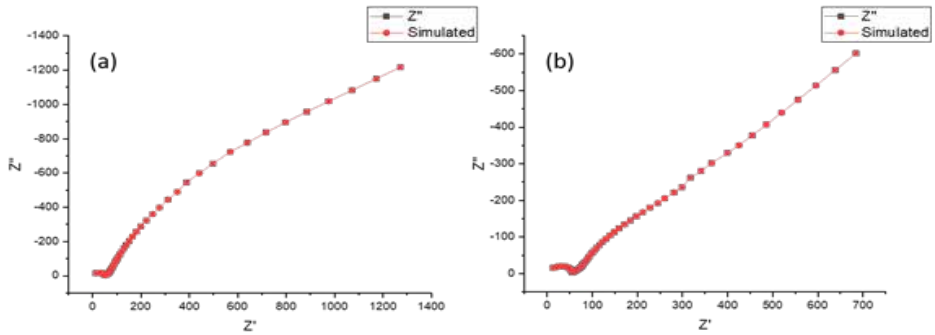

Fig. 7. Galvanostatic charge-discharge curves of (a) PS, (b) PS/GO nanocomposite.

Table 2. Table for specific capacitances and other circuit parameters for of PS and PS/GO.

Sample	Specific Capacitance (F/g)	R_s (Ohm)	R_{ct} (Ohm)
PS	2.78	10.77	4574
PS/GO	124	10.34	1958

the hydrophilicity nature of GO the ions can easily move to the electrode/electrolyte interface for PS/GO nanocomposite resulting in increased action site and high specific capacitance.

Conclusions

This study aimed to produce biodegradable starch/GO composite film. Therefore, natural biodegradable polymer starch were successfully extracted from potato. Glycerol is used as a plasticizer, and GO is used as a nanofiller with native starch to enhance the morphological, thermal, and electrochemical properties of starch-based nanocomposite films. GO/PS composites were prepared using a casting process as GO suspensions were stable in water. This stability was ascribed to the hydrophilic oxygen-containing groups and the thin layers. The abundant oxygen-containing groups of GO could form hydrogen bond interactions with starch. These interactions and the unidirectional, uniform dispersion of GO sheets in the PS matrix played essential roles in improving various properties. Furthermore, incorporating GO significantly

improves the nanocomposite's electrochemical performance. The PS/GO nanocomposite synthesized from a facile solution casting method may offer a sustainable route for synthesizing eco-friendly and transient energy storage devices.

Acknowledgments

The authors gratefully acknowledge the financial support from the Ministry of science and technology, Government of Bangladesh under the grant: 39.00.0000.009.14.011-20/ Phy's-578.

References

Bera M and Maji PK 2017. Graphene-based polymer nanocomposites: materials for future revolution, *J Poly Sci.* **1**(3): 94–97.

Bonardd S, Moreno-Serna V, Kortaberria GR, Díaz D, Leiva A and Saldías C 2019. Dipolar glass polymers containing polarizable groups as dielectric materials for energy storage applications. A Minireview. Polymers. **11:** 317.

Chandra S, Sahu S and Pramanik P 2010. A novel synthesis of graphene by dichromate oxidation. *Mat Sci Eng B-Adv.* **167:** 133–136

Ciszewski M, Mianowski A and Szatkowski P 2015. Reduced graphene oxide–bismuth oxide composite as electrode material for supercapacitors. *Ionics* **21:** 557.

Cole KS and cole RH 1941. Dispersion and absorption in dielectrics, alternating current characteristics. *J. Chem. Phys.* **9:** 341-351.

Dang ZM, Yuan JK, Zha JW, Hu PH and Cheng ZY 2013. High-permittivity polymer nanocomposites: Influence of interface on dielectric properties. *J. Adv. Dielectr.* **3:** 133-134.

Dang ZM, Yuan JK, Zha JW, Zhou T, Li ST and Hu GH 2012. Fundamentals, processes and applications of high-permittivity polymer–matrix composites. *Prog. Mater. Sci.* **57:** 660.

Deshmukh K, Ahamed MB, Pasha SK, Deshmukh RR and PR and Bhagat PR 2015. Highly dispersible graphene oxide reinforced polypyrrole/polyvinyl alcohol blend nanocomposites with high dielectric constant and low dielectric loss. *RSC. Adv.* **5:** 61933-61945.

Díez-Pascual AM, Sánchez JAL, Capilla RP, and Díaz PG 2018. Recent developments in Graphene/Polymer nanocomposites for application in polymer solar cells. *Polymers* **10:** 217.

Fan P, Wang L, Yang J, Chen F and Zhong M 2012. Graphene/poly(vinylidene fluoride) composites with high dielectric constant and low percolation threshold. Nanotechnology. **23:** 365-702.

Ge X, Li H, Wu L, Li P, Mu X, and Jiang Y 2017. Improved mechanical and barrier properties of starch film with reduced graphene oxide modified by SDBS. *J. Appl. Polym. Sci.* **133:** 44910.

Geng W, Zhao X, Zan W, Liu H and Yao X 2014. Effects of the electric field on the properties of ZnO–graphene composites: a density functional theory study. *Phys. Chem. Chem. Phys.* **16:** 3542.

Jammula RK, Pittala SH, Srinathb S and Srikanth VSS 2015. Strong interfacial polarization in ZnO decorated reduced-graphene oxide synthesized by molecular level mixing, *Phys. Chem. Chem. Phys* **17:** 17237-17245.

Khurram AA, Rakha SA, Zhou P, Shafi M and Munir A 2015. Correlation of electrical conductivity, dielectric properties, microwave absorption, and matrix properties of composites filled with graphene nanoplatelets and carbon nanotubes. *J. Appl. Phys. 118:* 044105.

Kim P, Jones SC, Hotchkiss PJ, Haddock JN, Kippelen B, Marder SR and Perry JW 2007. Phosphonic acid-modified Barium Titanate polymer nanocomposites with high permittivity and dielectric Strength. *Adv. Mater.* **19:** 1001.

Kim P, Zhang XH, Domercq B, Jones SC, Hotchkiss PJ, Marder SR, Kippelen B and Perry JW 2008. Solution-processible high-permittivity nanocomposite gate insulators for organic field effect transistors. *Appl. Phys. Lett.* **93:** 13-302.

Kumar P, Shahzad F, Yu S, Hong SM and Kim YH 2015. Large-area reduced graphene oxide thin film with excellent thermal conductivity and electromagnetic interference shielding effectiveness. Carbon. 94. 494–500.

Lin XY, Shen X, Zheng QB, Yousefi N, Ye L, Mai YW, and Kim JK 2012. Fabrication of highly-aligned, conductive, and strong graphene papers using ultra-large graphene oxide sheets. *ACS Nano.* **6:** 107-108.

Li R, Liu C, and Ma J 2011. Studies on the properties of graphene oxide-reinforced starch biocomposites. *Carbohydr. Polym.* **84:** 631–637.

Li Y, Zhou Y, Zhu Y, Cheng S, Yuan C, Hu J, He J and Li Q 2020. Polymer nanocomposites with high energy density and improved charge–discharge efficiency utilizing hierarchically-structured nanofillers. *J. Mater. Chem. A.* **8:** 6576-6585.

Maa T, Chang PR, Zheng P, and Maa X 2013. The composites based on plasticized starch and graphene oxide/reduced graphene oxide. *Carbohydr. Polym.* **94:** 63-70.

Malmir S, Montero B, Rico M, Barral L, Bouza R and Farrag Y 2018. Effects of poly (3-hydroxybutyrate-co-3-hydroxyvalerate) microparticles on morphological, mechanical, thermal, and barrier properties in thermoplastic potato starch films. *Carbohydr. Polym.* **194:** 357–364.

Maa T, Chang PR, Zheng P and Maa X 2013. The composites based on plasticized starch and graphene oxide/reduced graphene oxide. *Carbohydr. Polym.* **94:** 63- 70.

Nan CW, Shen Y and Ma J 2010. Physical properties of composites near percolation. Annu. *Rev. Mater. Res.* **40:** 131-51.

Samet M, Levchenko V, Boiteux G, Geytre G, Kallel A and Serghei A 2015. Electrode polarization vs. Maxwell-Wagner-Sillars interfacial polarization in dielectric spectra of materials: Characteristic frequencies and scaling laws. *J. Chem. Phys.* **142:** 194703.

Song S, Zhai Y and Zhang Y 2016. Bioinspired Graphene Oxide/polymer nanocomposite paper with high strength, toughness, and dielectric Constant, *ACS Appl. Mater. Inter.* **8**(45): 31264–31272.

Thomas S, Shanks R and Chandran S 2015. Design and applications of nanostructured polymer blends and nanocomposite systems, William Andrew, pp 1-576.

Tian M, Ma Q, Li X, Zhang L, Nishi T and Ning N 2014. High performance dielectric composites by latex compounding of graphene oxide-encapsulated carbon nanosphere hybrids with XNBR. *J. Mater. Chem. A,* 2: 111-144.

Usman A, Hussain Z, Riaz A, and Khan AN 2016. Enhanced mechanical, thermal and antimicrobial properties ofpoly(vinyl alcohol)/graphene oxide/starch/silver nanocompositesfilms. *Carbohydr. Polym.* **153:** 592-599.

Xia X, Wang Y, Zhong Z, George J and Weng 2017. A frequency-dependent theory of electrical conductivity and dielectric permittivity for graphene-polymer nanocomposites. *Carbon.* **111:** 221-230.

Xie S, Zhang B, Wang C, Wang Z, Li L and Li J 2013. Building up Graphene-based conductive polymer composite thin films using reduced Graphene Oxide prepared by γ-Ray Irradiation. *Sci. World J.* **7:** 954324

Yao PZ, and Zhou J 2015. Mechanical, thermal and dielectric properties of graphene oxide/polyimide resin composite. *High Perform. Polym.* **28**(9): 1033-1042.

Yousefi N, Lin XY, Zheng QB, Shen X, Pothnis JR, Jia JJ, Zussman E and Kim JK 2013. Simultaneous in-situ reduction, self-alignment and covalent bonding in graphene oxide/epoxy composites. *Carbon.* **59:** 406.

Yousefi N, Gudarzi MM, Zheng QB, Aboutalebi SH, Sharif F and Kim JK 2012. Self-alignment and high electrical conductivity of ultra-large graphene oxide/polyurethane nanocomposites. *J. Mater. Chem.* **22:** 12709.

Zhu Z and Guo W 2017. Frequency, moisture content, and temperature dependent dielectric properties of potato starch related to drying with radio-frequency/microwave energy. *Sci. Rep.* **7:** 9311.